Laser additive manufacturing for the realization of new material concepts

<u>Wilhelm Pfleging</u>, Juliana Solheid
Karlsruhe Institute of Technology, Institute for Applied Materials – Applied Materials Physics, Germany

i – Contents

14.1 – Introduction

In additive manufacturing processes, components are built up in layers from liquids, powders, wires or foils using chemical or physical processes. Direct energy deposition (DED) or powder bed fusion (PBF) can be used as additive manufacturing processes in which metal powder or wires are used to print dense metal layers on substrates or on freeform surfaces of existing components [1]. Metal powder (pure elements, element mixtures, master alloys) or metal wires are melted at high speed and instantaneously deposited in layers on respective metallic substrates. In case of the so-called laser cladding [2], this technology is generally used for applying coatings or for tool repairs. Compared to subtractive processes, additive processes save time and resources, as the material is only added where it is needed. Established steels, nickel-based alloys or titanium alloys are typically used. However, it is also possible to obtain completely new materials by in-situ alloying of powder mixtures or to create material gradients by changing the powder mixture composition during the build-up [3]. High entropy alloys (HEAs) represent a new research field for future applications. These are formed from a large number of elements, all of which are present in similarly strong concentrations e.g., alloys consisting of zirconium, niobium, hafnium, tantalum or tungsten [4]. The alloys formed can generally be single-phase as well as multi-phase mixed crystals. HEAs can often combine high strength and very good ductility. In-situ alloying offers the unique possibility of fast material screening for the future production of new metallic components with outstanding mechanical properties at high temperatures. For a long time, the manufacture of refractory alloys was limited to vacuum arc remelting because of their high melting points. With laser-based methods, these metals are locally melted by the focused laser beam and deposited additively. In addition to material development, additive manufacturing offers great design freedom in component design, which can be used, for example, for the development of load-optimized designs based on the bionic principle [5].

To add up to the versatility of additive manufacturing, laser post-processes can be used to modify the resulting surfaces of parts produced with such technology [6-9]. The different types of laser sources commercially available assure their suitability in a wide range of applications, with continuous wave (cw) lasers being often used for reduction of surface roughness, while pulsed lasers being applied in the modification of surface functionalities and to enhance the geometry accuracy. Even with the prospect of being able to replace certain steps of the additive manufacturing process chain, adopting laser post-processes as an additional step can also be proved beneficial when specific characteristics are required in localized areas of the final built components.

14.2 – Short Overview of AM Processes and Respective Applications

The technical term "Additive Manufacturing (AM)" describes a process of joining materials to create objects from three-dimensional (3D) model data, usually layer-by-layer, as opposed to subtractive manufacturing methods like milling or laser ablation. It is obvious that in case of large-scale 3D objects, subtractive manufacturing will in general produce a larger amount of material waste than established AM methods. However, in case of selective surface texturing or surface modification subtractive methods become more advantageous. Especially the combination of AM and laser ablation provide new opportunities in designing of 3D objects with local functionalities and biocompatibility as required for medical implants [9]. In section "14.4 – Laser Post-Processing of additive manufactured parts"

1

recent progress in this approach will be presented and discussed referring to biomedical surfaces and Ventricular Assist Devices (VAD).

Synonyms for AM are additive manufacturing, additive processes, additive techniques, additive layer production, layer production, and freeform production. Before focusing on AM of metallic parts let`s go back to the beginning of AM technology. The first AM technology is based on an invention and patent of Chuck Hull in 1984 describing the application "for Apparatus for production of three-dimensional objects by stereolithography", which is subsequently annotated as a stereolithography apparatus (SLA) [10]. In 1986, C. Hull founded 3D SYSTEMS emerging the worldwide first commercialized rapid prototyping system, i.e., the first 3D printer, in 1987, the SLA-1. The related process is based on a laser-induced photo-polymerization process, wherein a UV laser beam is scanned on a vat of photo-polymer resin. 3D prototypes are formed by curing the monomer resin layer-by-layer while in between each layer the build platform submerges deeper into the resin vat. Nowadays, the principle of this technology covers a broad scale range, from submicron range up to several meters. Regarding submicron technology the work of Kawata et al. [11] was a technical milestone enabling sub-diffraction-limit fabrication of micro-objects like the so-called micro-bull sculpture (Figure 1a). The new approach was to use femtosecond laser radiation and to initiate a two-photon photopolymerization with sub-diffraction-limit resolution as schematically described in Figure 1b by pushing the pulse energy close to the polymerization threshold. Already in 2015 the researchers from Oak Ridge National Laboratory (ORNL) were able to print cars (Figure 1c) or even buildings with up to a size of 11.5x3.7x4.0 m^3 [12]. The Shelby Cobra was printed using 20 % carbon fiber reinforced ABS material. During large-scale polymer deposition, polymer pellets were heated to near molten temperatures and extruded layer-by-layer onto an out-of-the-oven build platform.
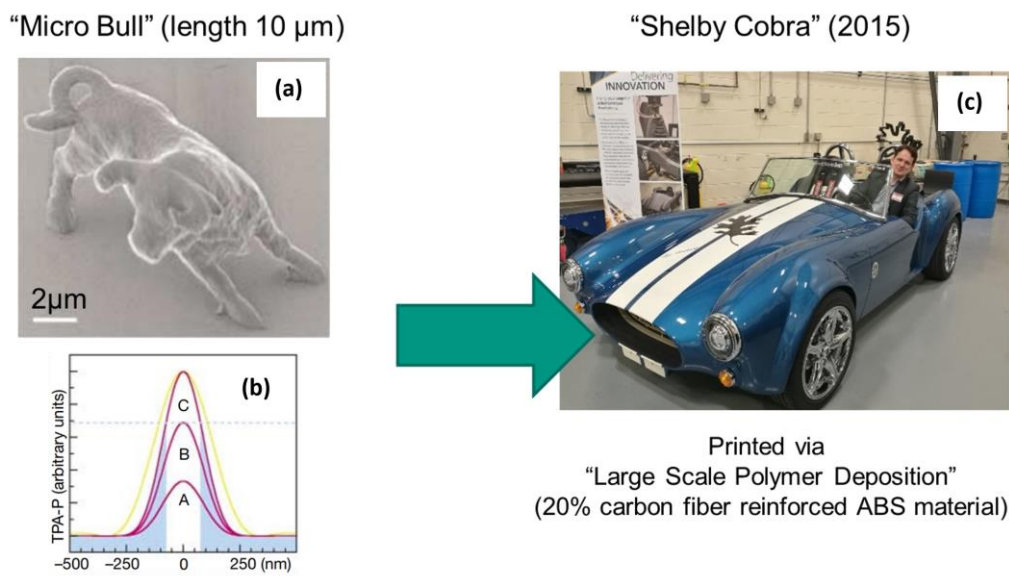

Figure 1: Scale range of AM technologies. (a) Microfabrication and nanofabrication at sub-diffraction-limit resolution by 2-photon–photopolymerization with (b) laser-pulse energy below (A), at (B) and above (C) the polymerization threshold (dashed line) [11]. (c) At Oak Ridge National Laboratory (ORNL) printed Shelby Cobra (est. 1965) by large-scale polymer deposition.

In addition to polymer, metallic alloys as material for AM technologies are of huge interest in research and development, since more than a decade ago. Laser cladding/coating and laser metal deposition (LMD) for repairing of damaged turbines and 3D metal printing for the rapid production of objects on a large scale became reliable technical approaches for small and medium batches.

2

In 2015, the Beijing University of Aeronautics and Astronautics demonstrated the 3D laser printing of a cockpit window frame assigned to a commercial aircraft (C919). The printing time for the frame took 55 days which is quite impressive considering that an aircraft manufacturer in Europe takes 2 whole years with a budget of about $2 million to just to develop the moulds for making similar frames [13]. The Comac C919 is China's first domestically built commercial aircraft. The Northwestern Polytechnic University (NPU) of China was producing within 25 days a five meter-long titanium central wing spar for the C919 passenger plane (Figure 2) [14]. The LMD system at NPU was developed in 2013 for inert atmosphere printing of components with sizes up to 5x2.5x0.6 m^3, with an accuracy of about 1 mm [15].

Figure 2: Selective laser sintering (SLS) for 3D printing of large scale objects made of titanium alloys for application in aircraft industry (a) C919 aircraft cockpit window frame [16], (b) 5 m high wing carrier [14].

The commercial aircraft manufacturer Airbus has been increasingly gaining the importance of laser sintering and melting of metal powders in aircraft manufacturing. The cabin bracket connector (Figure 3) is used in the Airbus A350 XWB [14].

Figure 3: The first titanium bracket connector produced using additive manufacturing on board the Airbus A350 XWB [17].

The bracket was additively manufactured using the so-called Laser Cusing technology (Concept Laser GmbH), which is in principle working like the laser powder bed fusion (LPBF). In the past, the cabin bracket connector was milled and machined out of aluminium alloy. Now it is a 3D printed part, which is made out of titanium powder material with a more than 30 % weight reduction. Mechanical milling of such aircraft parts leads 95 % material waste, while with LPBF the percentage of waste is only 5 %. In AM tools are not required to produce functional sample part thereby eliminating the tool and mould costs. This also helps in identifying early stage design errors and design optimization. In the past,

Airbus projected 6 months to develop such components, which could be reduced to 1 month by establishing LPBF.

The exact knowledge and reliable prediction of the component behaviour under the load conditions prevailing in the respective application are of essential importance for the establishment or broader application of AM technologies. The load-bearing capacity or the mechanical behaviour of additively manufactured metallic structures is, as in the case of conventionally manufactured components, largely determined by the microstructure and thus by the thermo-mechanical conditions during processing. In a direct comparison of these conditions, however, there are significant differences between additive and conventional manufacturing processes. For example, the volume of material that is temporarily in the molten state during processing is much smaller in relation to the component to be manufactured with the AM process than with casting or welding, for example. In addition, due to the layered production method, there is a constantly repeated heat input. As a result, different solidification conditions as well as different thermal histories, i.e., different temperature-time paths, are to be expected. However, regarding component weight and optimized stability properties under mechanical load a topology optimization for achieving an optimal material distribution is strongly recommended. Topology optimisation and selective laser melting was also applied during the manufacture of the above mentioned light-weight aircraft bracket by achieving 30 % weight reduction with an enhanced safety [18]. The use of construction principles from nature in technical applications, so-called bionic principles, is nowadays a common approach to enable lightweight constructions with optimized mechanical properties. In principle, material is mainly used where the greatest mechanical loads occur, while less material is distributed in places that have only a lower load leading to so-called cellular structures or materials [5].

Main types of additive manufacturing of metallic objects with the most prospects of product marketing are based on electron beam (EB) processes or laser beam technologies. However, a more general approach in classification of manufacturing technologies related "Additive Manufacturing (Metal)" is given in [1]. Based on this, but a significantly more condensed overview is given in Figure 4.
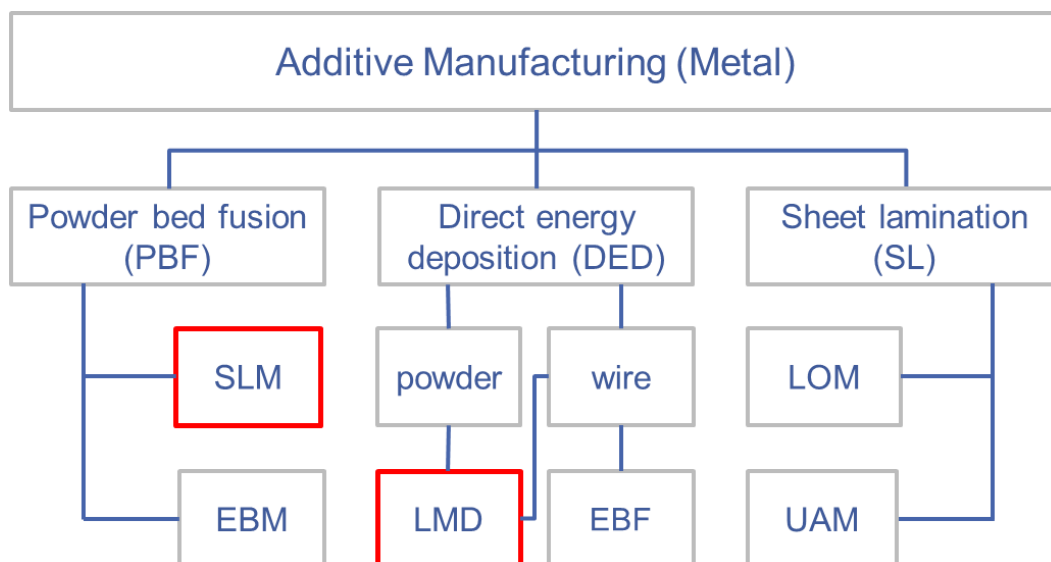

Figure 4: Overview of additive processes for metallic materials (EBM: electron beam melting, SLM: selective laser melting, LMD: laser metal deposition, EBF: electron freeform fabrication, LOM: laminated object manufacturing, UAM Ultrasonic additive manufacturing). The red-framed boxes are related to laser-based AM technologies.

4

Sheet lamination and especially Laminated Object Manufacturing (LOM) are derived from the principle of the first in 1991 commercialized additive manufacturing techniques involving layer-by-layer lamination of paper material sheets, which in advance were cut using a CO_2 laser [19]. Also complex-shaped 3D metallic parts have been made starting from laser cut metallic sheets and foils employing diffusion bonding, laser spot welding, brazing techniques, and ultrasonic welding (UAM).

More relevant in current research and development is the application of powder bed fusion technologies (PBF) and direct energy deposition technology (DED) using electron or laser beam as possible heat sources.

Two electron beam based AM technologies will be highlighted and shortly described due to their relevance in current AM applications:

- DED-EBF
- PBF-EBM

DED-EBF is an AM technology using a mobile electron beam gun and a wire feeder within a vacuum chamber to fuse a deposited bead of metal, one bead at a time layer-by-layer. High deposition rates of about 6.8–18 kg per hour can be realized for titanium or tantalum. However, the material selection is limited by the reliance on commercial sources of wire used by the process. One disadvantage is the slow cooling rate of the deposit within the vacuum environment and its potential effect on large grain growth and other metallurgical effects of the deposit. Advantages are that very large build volumes are possible and that the use of materials that are expensive, reactive, or of high melting points is possible due to the capability of high beam power and the high purity vacuum environment [20].

PBF-EBM is an AM technology that selectively consolidates metal powders such as titanium, Inco 718, and cobalt alloys to create 3D structures. Compared to conventional manufacturing processes, the EBM process is able to manufacture items with low volume and high value with reduced lead times. The method involves focusing an electron beam in a powder bed of metal particles to create a localized melt, followed by resolidification that enables complex geometries to be fabricated layer-by-layer. The EBM system consists of an electron beam gun, vacuum chamber, building tank, and powder distribution mechanism. EBM systems are able to achieve scanning speeds of up to 8000 m/s with an electron beam positioning accuracy of ± 0.025 mm and a single layer thickness in the range of 0.05 to 0.2 mm [21].
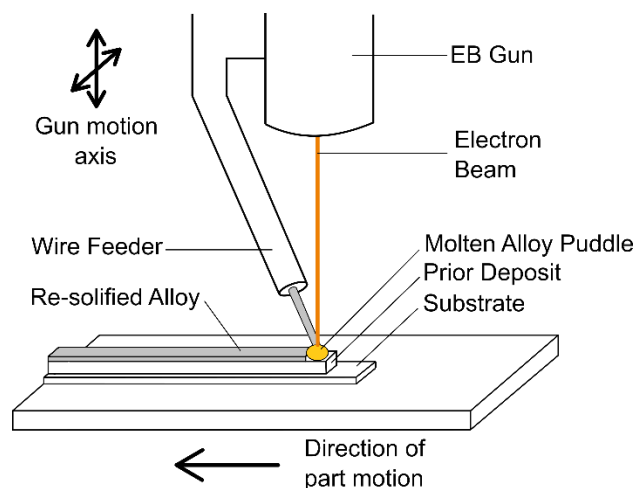

Figure 5: Schematic view of direct energy deposition process using e-beam and wire technology.

14.3 – Laser Additive Manufacturing

In the following, laser based AM technologies Selective Laser Melting (SLM) and Direct/Laser Metal Deposition (DMD, LMD) will be introduced with regard to typical process parameters and characteristics.

SLM (or LPBF) is operating under inter atmosphere (nitrogen, argon) in order to avoid oxidization of the metallic powder such as aluminum and titanium and to avoid impurities in the respective 3D metallic object. The type of SLM operation is schematically shown in Figure 6.

- **Laser power**: 400-1000W

- **Growing rate**: 88 cm³/h

- **Building chamber**: 280x280x365mm³

- **Atmosphere**: (Ar, N_2)

- **Layer thickness**: 20µm – 90µm

- **Powder grain size**: 15-45µm
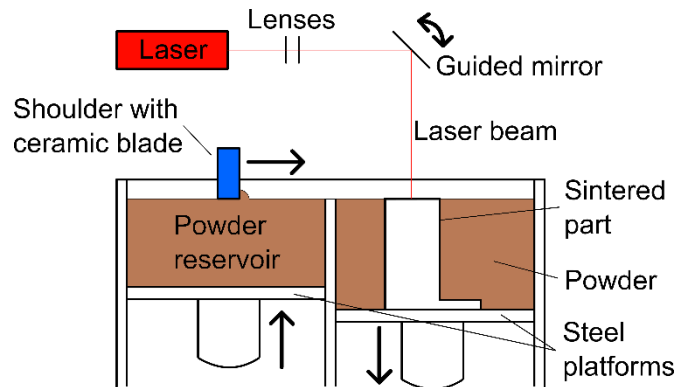
- **Roughness R_a** = 9-20µm (*as-built*)

Figure 6: Process parameters and schematic view of principle selective laser melting operation.

As shown in Figure 6, powder material with typically mean diameter values up to 50 µm is spread onto a building plate driven by a blade or a wiper mechanism. The space between the surface of the building plate and the bottom edge of this spreading mechanism defines the single layer thickness. This single layer thickness is typically smaller than 100 µm. In powder bed fusion the process parameters have to be carefully selected with regards to the single layer thickness and the selected type of material. After deposition of a powder layer a laser beam with an operation wavelength of about 1064 nm is focused onto the powder bed and is scanned along the powder surface in a sliced 3D CAD (computer-aided design) defined pattern. The scanning strategy is also an important task due to the fact that it has strong impact on the quality, micro-structure, and defect formation. Once a single layer is completed, the building platform is stepwise moved down and the procedure for a single layer formation is repeated until the 3D build process is completed. It is worth to mention that the laser beam exposure induces a melting depth into the previous layer to enable a full fusion of each layer into the previous (see also Figure 9). Consequently, the texture properties in the finished metallic part are less directional.

In Figure 6, the process parameters related to a commercial AM system (SLM 280, SLM Solutions Group AG [22]) are illustrated. The minimal achievable structure size is 150 µm with an as-built average surface roughness of 9 – 20 µm and a growing rate of up to 88 cm³ per hour. The material density of the final 3D object is in the range of 98.8 % up to 99.9 % of the pure alloy. It is also very common to apply a preheating platform depending on the process with adjustable temperature in the range of 20 up to 200 °C in order to reduce intrinsic mechanical stress formation.

The "Laser Metal Deposition" (LMD) process is also known as Direct Energy Deposition (DED), Direct Metal Depositon (DMD) or Laser Cladding. Previous applications of the process were limited to the processing of standard alloys (steel, titanium or aluminum alloys), e.g., for the quick repair of damaged

technical components or the application of protective layers. Technological and methodological progress is now opening up access to completely new fields of application such as "high throughput examinations" and "additive 3D production of samples and components" [23-26]. LMD can be used to create parts directly from a three-dimensional CAD model by applying materials layer-by-layer. This technology offers a high degree of flexibility due to the possibility of modifying an existing design (substrate) and manufacturing macroscopically extended components. During laser metal deposition, metal powder (pure elements, element mixtures, master alloys) is brought into the focus of a high-power laser beam (fiber laser; diode laser) at high speed, melted and instantaneously deposited in layers on a substrate or component. The effect of the laser beam on the substrate or layer surfaces can also be used to generate a small weld pool in a controlled manner, in which, for example, hard materials such as TiC are to be dispersed [27]. This makes alloys and metal-ceramic composites accessible (see chapter "14.5 – Material Screening"). After rapid solidification, a material layer with a thickness of up to a few hundred micrometers is formed. The type of LMD operation is schematically shown in Figure 7. By repeatedly scanning the surface with the laser, multiple layers can be deposited on top of one another according to a given CAD/CAM model and larger samples can be produced. The chemical compositions, the microstructures and the resulting material properties can be changed in a controlled manner from layer to layer. The materials that build up the individual layers are very homogeneous with an adapted process management and can be characterized very precisely, e.g., with chemical analysis. The most promising alloys or composite materials for the respective applications can thus be efficiently determined and processed into larger, complex-shaped components with the LMD system through additive 3D manufacturing [26]. Typical process parameters are given in Figure 7. It is obvious that LMD in comparison to SLM is not as precise due to the higher layer thicknesses but enables a three times higher deposition rate. Furthermore, LMD offers outstanding prospects to develop new materials and components with designed properties.
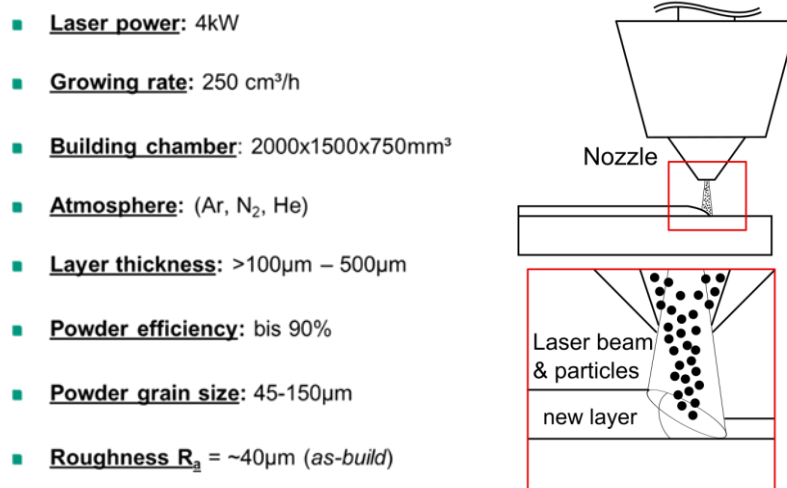

- **Laser power**: 4kW
- **Growing rate**: 250 cm³/h
- **Building chamber**: 2000x1500x750mm³
- **Atmosphere**: (Ar, N_2, He)
- **Layer thickness**: >100µm – 500µm
- **Powder efficiency**: bis 90%
- **Powder grain size**: 45-150µm
- **Roughness R_a** = ~40µm (*as-build*)

Figure 7: Process parameters and schematic view of principle "selective laser metal deposition" / "direct metal deposition".

14.3.1 – Fundamental Aspects of Laser Material Processing

Laser material processing is a technique based on irradiating a substrate surface with laser radiation at high intensities (>10^5 W/cm^2). The optical energy is absorbed by the electronic system which subsequently transfers energy into the phonon system until thermal equilibrium is reached. For laser pulse lengths above 100 ps (10^{-12} s) the thermalisation of electrons and phonon occurs almost

instantaneously and processes are denoted as thermal laser processing. Laser additive manufacturing technologies for metals based on SLM and LMD are always thermally-driven due to the required melting processes. Generally, a good understanding of heat transfer fundamentals is of great importance to comprehend the laser/material interaction and select the most appropriate system and parameters for a given application [8].

Initially, it is important to describe the characteristics of the laser beam as heat source. Laser beams with Gaussian intensity profiles are widely adopted and can be expressed as a heat flux as shown in Equation (1):

$$Q'' = \frac{2AP_w}{\pi R_w^2} e^{\frac{-2(x^2+y^2)}{R_w^2}} \tag{1}$$

Where Q'' is the surface heat generation term, R_w is the distance from the center of the heat source, A is the laser absorption coefficient, and P_w is the laser power.

The generated heat interacts with the material in question. A simplified heat transfer equation to describe the heat dissipation within the part being processed is expressed in Equation (2):

$$\rho C_p \frac{\partial T}{\partial t} = k\nabla^2 T \tag{2}$$

where k is the effective thermal conductivity, C_p and ρ are the effective specific heat capacity and density of the material, respectively.

Although, not all the optical laser energy is transformed into heat that will affect the process and properties of the final part, since heat exchanges with the environment through convection and radiation (Stefan–Boltzmann law) are almost impossible to be avoided. Both heat losses can be described by Equation (3) for the former and (4) for the latter:

$$Q_{conv} = h(T_{amb} - T) \tag{3}$$
$$Q_{rad} = \varepsilon\sigma(T_{amb}^4 - T^4) \tag{4}$$

with h the convective heat transfer coefficient, ε and σ the surface emissivity and the Stefan-Boltzmann constant, respectively.

During several laser materials processing, phase changes occur and the thermo-physical properties of the material should be assessed accordingly.

It is worth to mention that for ultrafast laser radiation the above mentioned concept has to be modified by introducing a so-called two-temperature model [28]. A main advantage of using ultrafast laser processes is that melting or heat affected zones can be almost avoided by minimizing thermal effects [29-31]. Therefore, ultrafast laser radiation is a preferred manufacturing tool for surface texturing and functionalization with structure details down to the nanometer range.

14.3.2 – LMD Process Characteristics

The main objective is to refine metallic surfaces or to gain new functions through a coating. For this purpose, the metallic surface is melted on in a locally limited manner with intense and focused laser radiation. Particles or powder mixtures are then sprayed into the molten bath. In this approach, the layers below are also melted again in order to achieve a good adhesion and tight transition. The layered coating leads to an intrinsic heat treatment of the underlying areas. First of all, the melting temperature is reached on the top layer and the layers below experience a repeated temperature control, which in some cases can reach the melting temperature. Thus a periodic heating of the individual layers takes place. This means that the microstructure and the internal stress of the lower layers will be adjusted depending on the process parameters and the number of layers. The main process characteristics of laser metal deposition (LMD) are as follows:

- Transport of metal powder (pure elements, element mixtures, master alloys) at high speed

- Melting in the focus of a high-power laser beam
- Locally thin melt pool on substrate or layer surfaces
- Layered structure on a 2D/3D substrate/component
- Alloying and dispersing (e.g., hard materials)

Hereby the nozzle configurations for guiding the powder material plays an important role regarding the requested application scenario. Conical ring nozzles provide a small powder focus diameter suitable to establish 0.5mm width tracks. Another design is denoted as multi-jet nozzle with a large powder focus to enable melt tracks with a width in the range of 1-3 mm and typically applied laser powers above 1000 W. This nozzle design is suitable for 3D positioning of the laser and powder injection relatively to the building platform. Finally the lateral nozzle arrangement which enables an efficient powder application but which is strongly depending on the building and laser scanning direction. The later nozzle design is not suitable for a flexible building up 3D components.

14.3.3 – Defects, Structures, and Textures

During laser AM a huge number of different types of defects can be observed. In the following list the common observed defects are listed and shortly described:

- During solidification, gas bubbles can become trapped in the molten bath, which are caused by excessive stirring of the molten bath, porosity in the powder raw material or the evaporation of alloying elements and can lead to the formation of gas pores.
- Rapid solidification of the weld pool can lead to trapped porosity as the gas does not have enough time to exit the weld pool.
- Contraction cavities, so-called balling, can form when isolated pockets of liquid solidify separately from the remaining melt. The contraction stresses during the solidification of the terminal liquid are sufficient to pull the semi-solid material apart and create a contraction cavity (Figure 8).
- Incorrect surface preparation can lead to contamination of the weld pool, which affects the surface tension and the adhesion of the coating to the substrate
- Laser scan overlap mismatch can result in porosity in the overlap region if the deposit is excessively large as this reduces the contact angle and prevents the complete merging of adjacent lines.
- Residual stresses, hot and solidification cracks by volume change or shrinkage due to solidification
- Pore formation due locally high laser absorption, e.g., at hatch turning points (Figure 9a).
- Layer delamination due to heat accumulation and residual stress release
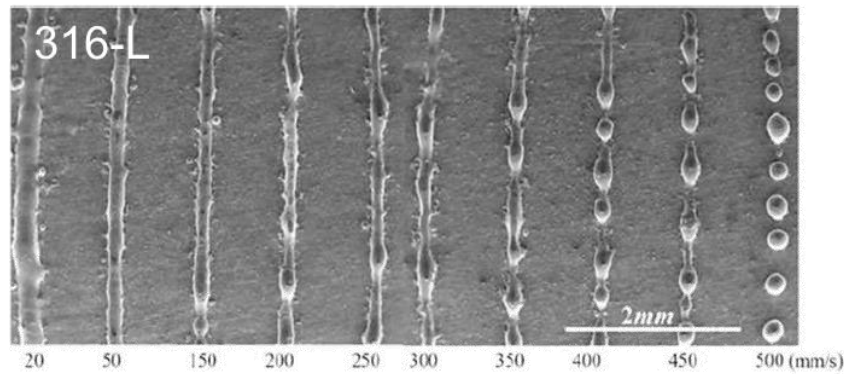
9

Figure 8: SEM images showing the balling characteristics of single scan tracks under different laser scan speeds [32].

Normally, due to orientation-dependent properties, such as the interface energy between the solid and liquid phase, the crystal growth parallel to the heat dissipation would take place in the direction of <001> for metals with a cubic structure, i.e., in the direction of the temperature gradient. This is the direction of crystallization with the greatest growth rate. When the laser is slowly scanned over the surface, a crystalline and columnar-like growth is caused towards the substrate. With increasing laser advance speed, the alignment of the microstructure growth will then be increasingly inclined with respect to the substrate normal. The grain size, on the other hand, essentially depends on the cooling rate. The resulting texture can also be influenced by varying the laser scan filling direction from layer to layer (Figure 9a). The fact that the underlying layers can be melted again (Figure 9b). creates a new structure with a disruption of the preferred texture alignment.
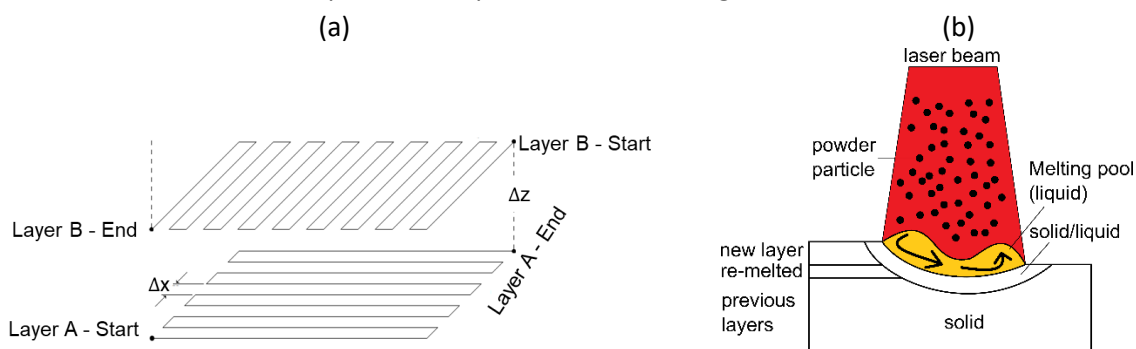

Figure 9: Process parameters disturbing a preferred texture grow in laser AM. (a) Laser scanning and hatch strategy. (b) Impact of Marangoni convection during laser processing.

Another important factor that influences the structure is the Marangoni convection (Figure 9b). The Marangoni convection is derived from the temperature dependence of the surface tension of the melt. The Gaussian intensity distribution of the laser causes a temperature profile on the melt. The surface tension depends on the temperature. If the surface tension decreases with increasing temperature, i.e. if it has its minimum in the center of the weld pool, then a movement of the melt towards the edges of the melt pool is caused on the surface. The Marangoni convection thus causes a melting bath turbulence, which in turn influences the texture in the later resolidified material.

Local adjustment of the microstructure and texture can be simply realized by controlling of laser power during LMD process as shown in Figure 10. The average grain size is in the range of 80 µm while applying a low laser power of 400 W, but the grains are less columnar crystalline. The texture is less pronounced with regard to <101> parallel to the building direction (BD). Adjusting the process parameters to higher laser power (1000 W), on the other hand, causes a significant increase in the

10

grain size, resulting in an average diameter of 235 µm. At the same time, the intensity of the <001> texture in relation to the BD is increased from 1.9 to 3.7. However, the cubic formation of the crystals is lost due to the rotation of the scanning direction from layer to layer (see Figure 9a) in successive layers used in the case of this sample. In the transition areas regarding the change in laser power, no defects such as pores, delamination or keyholes could be detected as possible indications of insufficient or excessive melting. The transition from the completely globular to the completely columnar-crystalline microstructure in the lower area of the sample takes place over a distance of approximately 400 µm and thus takes place over several layers. In contrast, the transition from columnar crystalline to globular microstructure appears to be significantly sharper, with the <001> texture being lost. Complementary hardness mappings confirm the basically very steep transitions between areas of high hardness (400W) and low hardness (1kW), whereby differences between the respective transition areas could not be resolved. The competing effects from the solidification parameters (thermal gradient and speed of the solidification front) and epitaxial growth as well as molten bath turbulence associated with Marangoni convection (see Figure 9b) certainly play an important role.
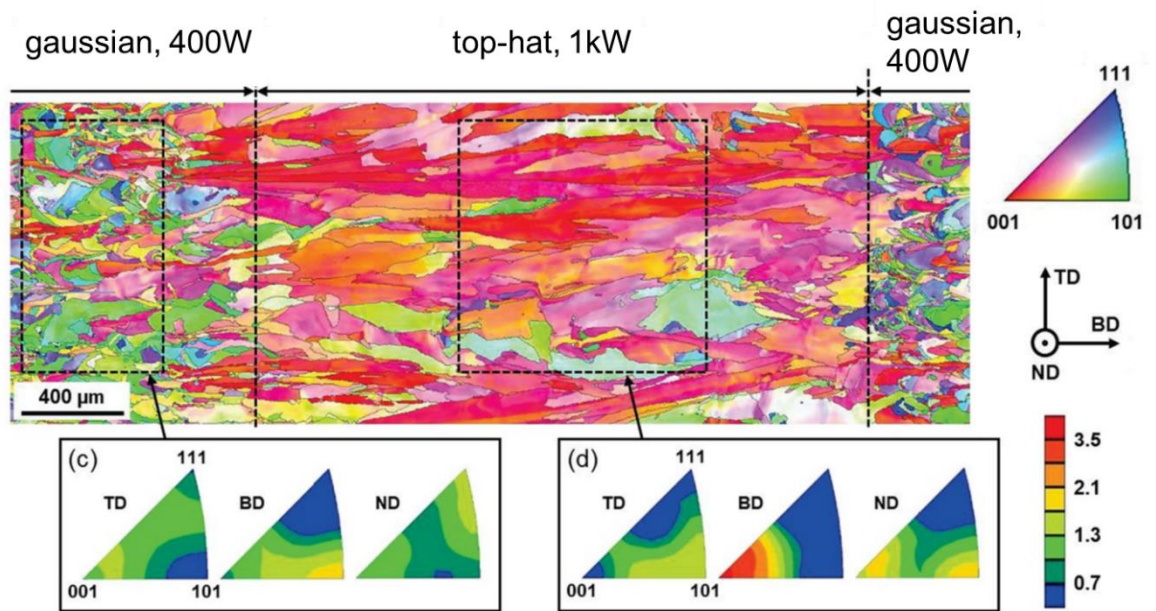

Figure 10: Microstructure analyses for a LMD produced X2CrNiMo17-12-2 steel sample by applying different laser power. The inverse pole figure mapping reveals that two different types of microstructures were formed. A fine-grained microstructure was obtained for low laser power (400W) while a columnar-grained coarse microstructure was achieved for high laser power (1000W). Also the respective textures in building direction (BD) differ significantly showing a strong <001> intensities for the columnar-grained material and much weaker intensities for the fine-grained regions [33].

14.4 – Laser Post-Processing of additive manufactured parts

In this section, laser-based post-process for improvement of surface quality by roughness reduction, termed laser polishing, and for modification of surface functionalities, named surface functionalization will be introduced with regard to typical process characteristics.

The laser polishing consists of irradiating the part's surface with a laser beam, thus generating a molten layer that is redistributed and resolidified to create a surface with lower roughness [34, 35].
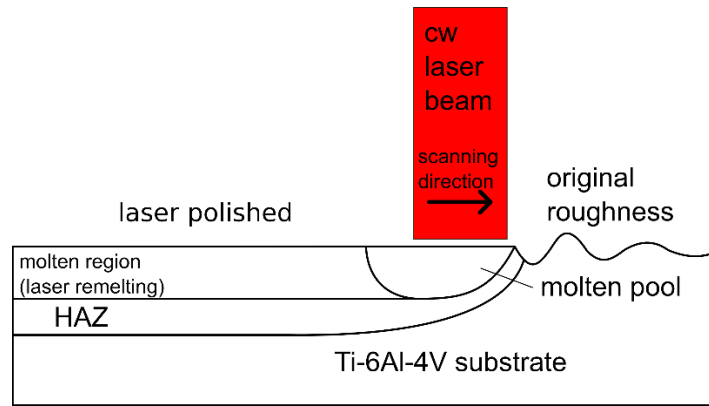
Figure 11: Schematic of the polishing process on the surface of the additively manufactured Ti-6Al-4V part using the continuous wave (cw) laser beam.

As shown in Figure 11 , a continuous wave laser with an operation wavelength of about 1064 nm scans the surface of the workpiece submitted to the laser polishing. Typically the mean laser spot diameter has a value of 100 μm, which can easily be increased by altering the laser focusing offset. Other process parameters that highly influence the processing outcome are the laser scanning speed, hatch distance, and laser power. Significant surface roughness reduction, from 6.9 μm to 0.8 μm, were obtained by repeating the laser polishing processing three times with laser power of about 300 W, scanning speed of about 1200 mm/s, and hatching distance of about 50 μm for a laser beam with diameter of 100 μm. It is worth to mention that the process is also characterized by deep melted and heat affected zones (HAZ) with consequent microstructural changes that affect the mechanical properties. Thermal models can be applied for a fast assessment of the dimensions of the melted zones and the heat-affected zones (Figure 12).
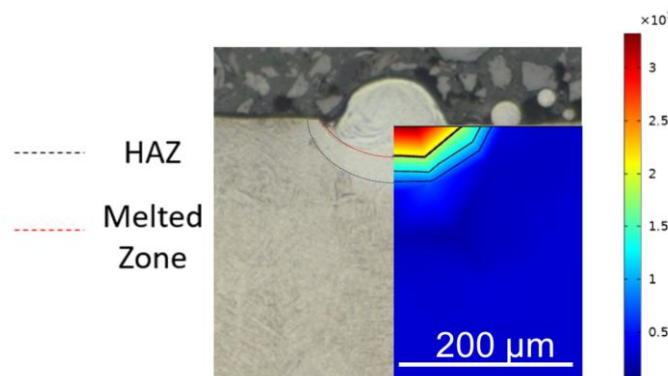

Figure 12: Comparison of the molten pool and HAZ morphology: cross section of a laser generated melt pool in AM Ti-6Al-4V and numerical simulation of the laser generated temperature field. Extracted from [8].

The work on modeling of the laser treatment process also include simulations of the mentioned specific features of the lasers parameters to predict the melt pool geometry and free surface characteristics to make a comparison with the experimental optimization.

In order to understand the microstructure evolution during laser remelting or heat treatment of titanium and its alloys to be produced in frame of the SLM or LMD processes, the thermal models can also be coupled with a metallurgical models to predict the grain size and phase fractions on the assessed heat-affected zones. Finally, experimental studies needs to be correlated with the evaluation of the material hardness and residual stresses after the laser treatment.

The laser functionalization process consists of modifying the surface of a workpiece to obtain characteristics that will serve for different purposes in terms of applications. Ultrafast lasers have been

widely used for the functionalization of metallic parts for their versatility in terms of process parameters and highly controllable ablation rates. When compared to continuous wave lasers normally used for laser polishing, the mean laser spot has a reduced diameter with values of about 60 μm, which can also be increased by altering the laser focusing offset but in considerably smaller ranges due to the Rayleigh length. The remaining process parameters that highly influence the processing outcome are the same as in the laser polishing, namely laser scanning speed, hatch distance, and laser power, with the addition of the pulse duration parameter. With this kind of technique, distinct structures can be applied onto the surface of the parts, which result in varied behaviours. Two types of structures were investigated in SLM built Ti-6Al-4V at various stages of the process chain, including after laser polishing, and different functionalities were assessed. The processing parameters adopted were the average laser power of about 4 W, scanning speed of 400 mm/s, pulse duration of around 450 fs, and repetition rate of 1000 kHz. The resulting structures presented nano-sized ripples and porous topographies and were obtained by repeating the process with the described parameters 1 and 5 times, respectively. For both surfaces a highly hydrophobic functionality was achieved with contact angles above 100°, while surfaces previously submitted to laser polishing presented contact angle of around 60° [9].

Due to current research work already an expertise in the field of laser modification of titanium and its alloys regarding control of biomedical aspects could be achieved [9, 36, 37]. The proposed laser post-processes for smoothening and texturing can be applied to ventricular assist devices (VAD), which have the potential to be 3D manufactured by SLM or LMD with improved material properties. The design of one type of centrifugal VAD is presented in Figure 13. Based on the results obtained in the laser post-processing investigations, the laser polishing is a suitable technique for the fast smoothening of the upper and down shells, while maintaining the desired biocompatibility of titanium and its alloys [9]. Still preserving the biocompatibility feature, the laser texturing is a suitable option for processing the surfaces of the rotor, in which hydrophobic characteristics are desired.
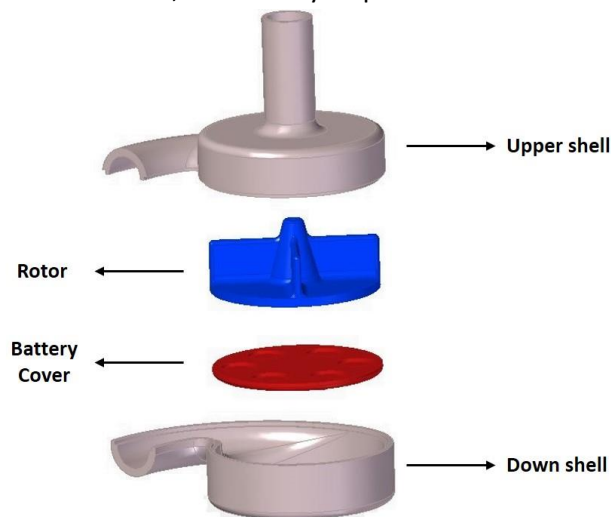

Figure 13: Exploded view with the main components of CARoL centrifugal VAD.

For a throughout investigation of the suitability of AM techniques for the manufacturing of VAD, the CARoL (Cardiac Assistant Recovery of Life) centrifugal blood pumps [38] were printed using a titanium alloy "LaserForm Ti Gr23 (A)" (3D Systems, Leuven) with high strength and biocompatibility. The SLM machine used was a DMP Flex 350 and the outcome is presented in Figure 14. To manufacture the chosen VAD via SLM without altering its design, the abundant use of supports structures are necessary due to the occurrence of several overhang areas with critical angles. Even when the limit angle of 45°

is obeyed, the use of support structures are justified by the need of dissipating the heat and avoiding the warping that can occur due to the dimension of the part. These support structures must be removed from the parts manually and sometimes with great effort, which affects considerably the resulting surface quality and dimensional accuracy, as shown in Figure 14b. Commonly, mechanical operations such as sandblasting, grinding, and machining are adopted as post-processes, although the use of non-conventional processes has increased significantly over the years.

Hemodynamic tests of the centrifugal blood pumps are going to be performed for the evaluation of the suitability of AM parts and advanced titanium alloys with adjusted materials properties and surface functionalities.
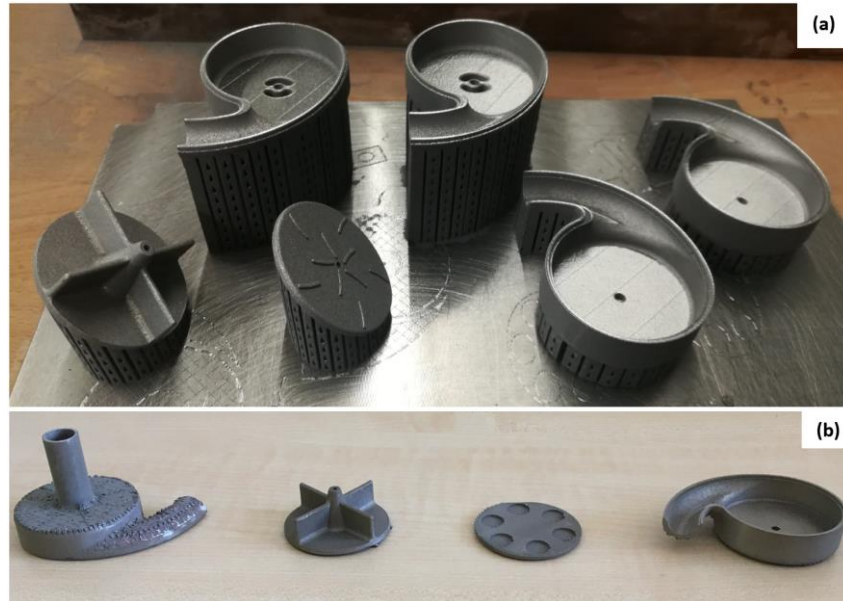

Figure 14: (a) CARoL VAD on the building platform displaying the supports structures necessary for their production via SLM. (b) CARoL VAD main components after heat treatment and operations for building platform and support structures removal. The rotor and the shell have a diameter of 43.6 mm and 48 mm, respectively.

14.5 – Material Screening

Recently, however, laser metal deposition (LMD) (Figure 15a,b) has been developed very successfully as a highly suitable method for high-throughput screening of alloys and at the same time for additive 3D manufacturing of larger components [23-25]. With the LMD process, numerous material variants with a wide variety of chemical compositions and microstructural designs can be combined within a single sample or component.
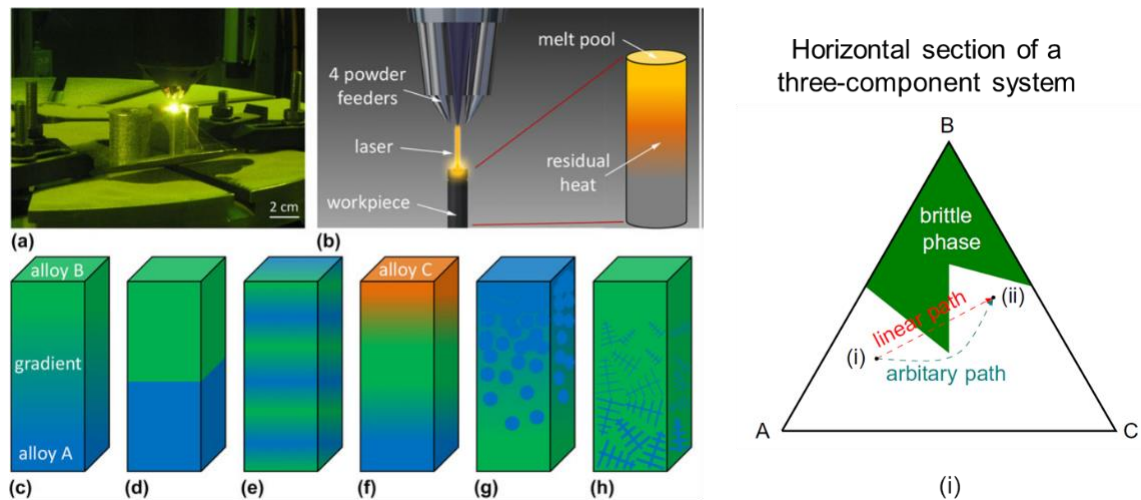
Figure 15: (a) LMD process for producing gradient alloys. (b) Schematic view of the LMD process. (c–h) Schematics of some of the different compositionally graded alloys that are possible using LMD process. These include the formation of gradients from one alloy to another and the formation of metal matrix composites (g,h). (i) Schematic view of a ternary phase diagram showing possible gradient paths from one alloy to another across a three-element phase space. Several routes are possible, based on factors such as the avoidance of brittle phases [39].

As previously described, the samples/components are built up individually by successive individual layers. Each layer can be individually adjusted in terms of its chemical composition and microstructural characteristics. Only small layer thicknesses of 0.3 to 0.6 mm are required for the high-resolution analyzes. The LMD process can be automated and carried out quickly in the sense of a high throughput process. Another very big advantage of the LMD method is that, thanks to the high material deposition rates of up to 1.5 kg per hour, large volumes of material can also be produced in a short time, and therefore larger components can be realized. The methodical advances in LMD control and regulation thus also make additive 3D manufacturing fully accessible. Alloys and metal-ceramic composites (Figure 15c-h), which turn out to be particularly suitable for certain applications with the high throughput method, can be processed into larger components with the same LMD system. This means that the material screening approach can be directly coupled with laser additive manufacturing for the production of larger components. In order to avoid brittle phases during LMD process, phase diagrams should be used as guiding maps for the LMD process (Figure 15i). The red line in Figure 15i indicates the simple approach for moving from one alloy to another by linearly changing the powder composition during LMD. In the presented case, the brittle phase will be crossed leading to crack formation in the deposited component. To avoid the brittle phase and to achieve a well designed object with the properties of the alloy end members, the powder composition has to be adjusted during LMD as described by the green line (Figure 15i). In the following three examples of material screening presented, namely the development of composite materials, graded alloys, and high entropy alloys (HEA).

14.5.1 – Composite Materials

Ti6Al4V is one of the most established titanium alloys in AM. For achieving an increase in mechanical strength especially for use in environments with elevated temperatures up to 500°C the development of composite materials based on Ti6Al4V matrix with embedded TiB_2 and TiC was investigated by using LMD [40]. For this purpose a powder mixture (Figure 16a) – a so-called powder blend - consisting of Ti6Al4V and a small amount of B_4C particles (0.5-1.5 wt) was sprayed into the laser generated melting pool. A chemical reaction as illustrated in Figure 1b took place by forming TiB and TiC microstructures

within the titanium alloy matrix. In comparison to the standard Ti6Al4V alloy a severe grain refinement could be achieved finally leading to an increase in modulus of elasticity and micro-hardness Figure 16b. The cross section analysis (Figure 16c) of the generated composite shows no imperfections like pores or cracks along the entire building path.
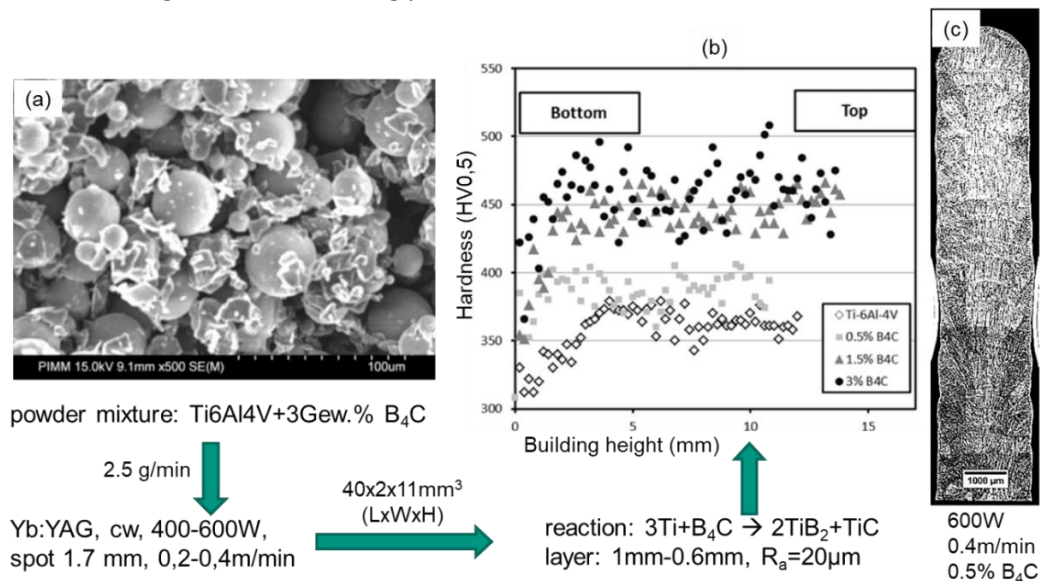

Figure 16: Process sequence for LMD fabrication of Ti6Al4V-B4C composite with outer dimension of 40x2x11 mm³ (length x width x height). Typical Yb:YAG laser and process parameters are illustrated (laser power, spot size, scan speed). Single layer thicknesses are in the range of 0.6-1 mm. (a) SEM picture of Ti-6Al-4V / B₄C (3wt.%) powder blend. (b) Microhardness values of LMD composite material as function of building height and B₄C content in powder blend (c) Cross-sections of manufactured walls for 0.5wt.% B₄C in powder blend [40].

14.5.2 – Graded Materials

In the LMD process, powders of different particle size distribution and topography are used, each of which also requires different nozzle concepts (e.g., annular gap, bores). The use of small powder sizes in the range below 100 μm, e.g., 40-90 μm, is recommended for creating gradient layers or material alloys of varying composition. The powder flow is in general guided coaxially to the laser beam.

In current state of research in the field of laser additive manufacturing of titanium alloys a main topic is the evolution and determination of grain texture with its impact on mechanical properties such as hardness, ductility, yield strength, and elongation at fracture [41]. Numerical simulation can be used to describe the grain growth during laser additive manufacturing process. The grains are found to be elongated and columnar after solidification which gives arise to anisotropic properties [42]. For as-deposited titanium alloys, defined phase composition transformations could be observed along the deposition direction as well as a change in micro-hardness as function of structure height [43]. During laser processing low or high cooling rates up to 10^7 K/s can be used to design the surface but also the entire material properties along three dimensions. This type of functional grading based on the microstructure control for each single layer can be coupled with a change in composition and phase along the building direction.

A prominent LMD example for the connection of steel alloys with different properties is combination of 304L stainless steel (Fe68Cr20Ni10Mn1Si0.3) with Inconel625 (IN625) [3]. While 304L is of lower cost and mass, IN625 shows enhanced mechanical strength and corrosion resistance at elevated temperatures. These both materials seems to be ideal for establishing tools with graded composition due to the fact that both alloys have a face-centered cubic (fcc) crystal structure from melt to room temperature without allotropic phase transformations. Furthermore, the main components of the

alloys such as Fe, Cr, and Ni show good solubility. During the LMD production of the graded component (Figure 17a,b) the powder blend composition containing 304L and IN625 particles was gradually changed along 24 layers (Figure 17a).
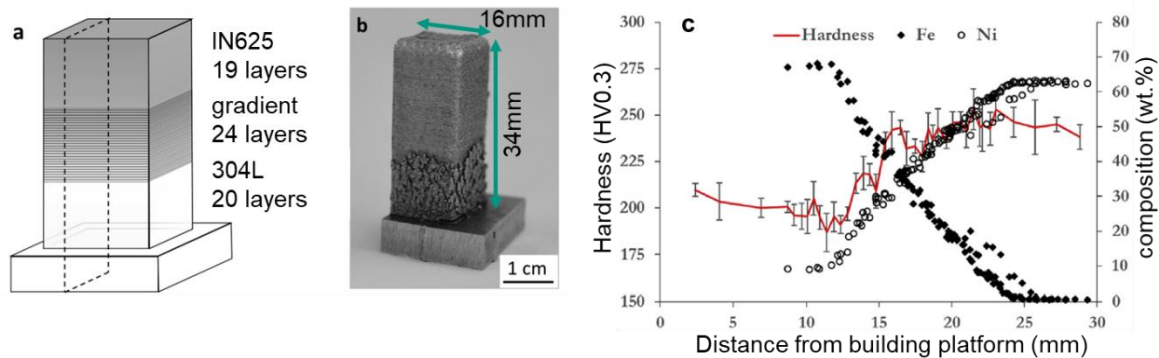

Figure 17: (a) Schematic of gradient alloy specimen. Dotted line shows where part was cut for subsequent elemental and hardness measurements. (b) Photograph of specimen after LMD fabrication. (c) Microhardness of the gradient alloy overlaid on Fe and Ni composition [3].

20 layers of pure 304L were deposited onto the building platform and after the graded section of 24 layers pure IN625 was deposited for 19 layers each layer with a thickness of about 500 µm and a total component height of 34 mm (Figure 17b). The Fe and Ni composition gradually changed as expected (Figure 17c) and an increase in hardness of about 50 HV above the manufacturer's specifications of the starting material could be achieved. However, a slight drop in hardness at the beginning of the graded zone could be detected which is be due to crack formation related to the formation of mono-carbides (containing Mo and Nb) at the transition zone from the 304L to the gradient. It is obvious as described earlier that a simple linear change in powder blend composition is in general not an appropriate procedure for establishing graded materials and a controlled bypassing of possible brittle compositions becomes necessary (see Figure 15i). As shown in (Figure 17c) a slight decrease in hardness is also observed in the upper range of the component which is caused by enforced grain grow by heat accumulation along the tip. The maximum hardness was achievement in the center of the gradient zone (Figure 17c).

14.5.3 – High Entropy Alloys

Compared to the classic concept of single-base alloys such as steels or Ni superalloys, there has been an intensive search for new alloys based on the concept of high entropy alloys (HEA) for around 15 years. According to this concept, several elements are mixed together in almost equal proportions. The term entropy alloy is derived from the high configuration entropy resulting from the random mixing of the elements in the alloys. When developing alloys, researchers focused on the corners of a phase diagram to develop a conventional alloy. These alloys only take up a small part of the design space in the phase diagram. The focus at HEA has now been shifted to the central region. There is still no uniformly recognized definition of HEAs [44]. Originally, alloys with high entropy were defined as alloys that consist of at least 5 elements with an atomic fraction of 5 to 35 atomic percent. However, another definition states that for being denoted as HEA it is necessary that those alloys only form mixed crystals without intermetallic phases which reflects the general meaning of providing high entropy. Therefore HEAs with less than 5 elements can be created. But why dealing with HEAs? The main reason is the superior mechanical performance at elevated temperatures in comparison to the well-known steels and superalloys [44].
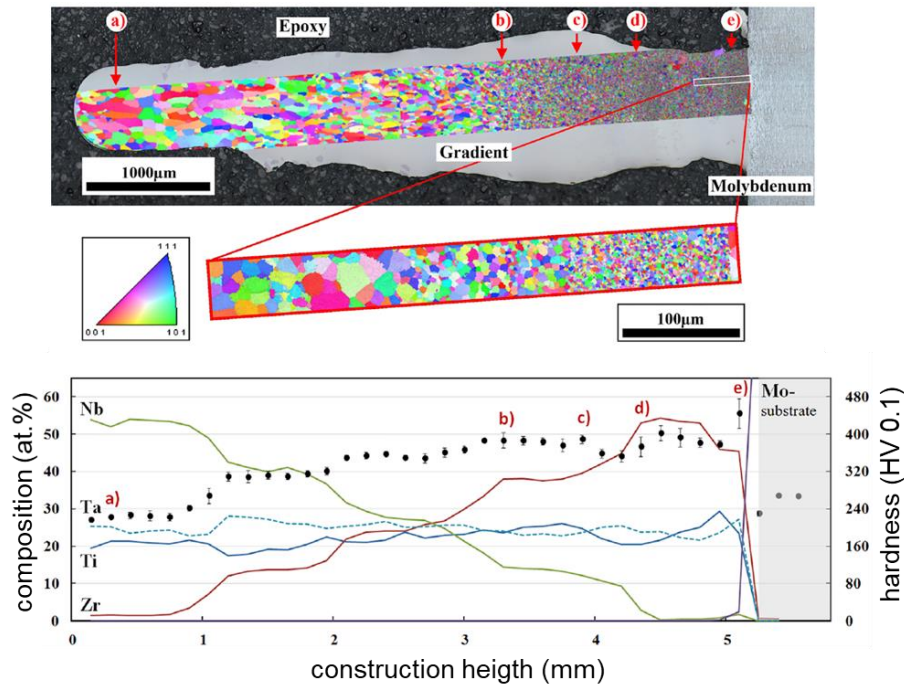
Figure 18: Top: SEM image with an overlaid color-coded grain orientation map of a cross-section of a LMD produced structure (building platform on the right side is made of Mo). The colours in the grain orientation map indicate the crystal orientations (bcc unit cell) parallel to the building direction (BD) displayed in the stereographic triangle (middle left). Bottom: Composition gradient and respective micro-hardness along building direction [45].

In-situ alloying by LMD provides unique prospects regarding the development of new and advanced HEAs as shown by recent research activities [4, 45, 46]. Besides the formation of new HEAs by establishing a defined composition [46] it is also possible to realize HEAs with graded composition as shown for the very first time in 2019 by Dobbelstein et al. [45]. In that work they synthesized TiZrNbTa HEA by varying the Nb and Zr concentration along building direction as shown in Figure 18. The compositionally graded material was built by LMD using five powder blends and by changing the chemical composition from Ti25Zr50Nb0Ta25 at building platform to Ti25Zr0Nb50Ta25. Due to the formation of secondary phases a solid solution strengthening could be induced resulting in an micro-hardness increase with the proportion of Zr (Figure 18, bottom). The increase in grain size at the end of construction is again related to heat accumulation which is increased with increasing structure height.

14.6 – Conclusion

With laser additive manufacturing, i.e., selective laser melting (SLM) and laser metal deposition (LMD) extensive research work on development of 3D components for different type of application was performed. While SLM is most appropriate for establishing devices with high accuracy as required for the development and production of implants such as VAD components, LMD provides new opportunities to develop new materials with designed properties such as graded materials or high entropy alloys. The chemical compositions of the alloys and the process engineering manufacturing conditions can be varied very flexibly within a wide parameter range. This allows phase and microstructures as well as local chemical compositions and the resulting physical and mechanical properties to be researched efficiently. In addition, ceramic powders can be introduced to produce composite materials. The chemical compositions, the microstructures and the resulting material properties can be changed in a controlled manner from layer to layer. The most promising materials

18

for the respective applications can thus be efficiently determined and processed with the LMD system into larger, complex-shaped components. LMD is a powerful tool to produce 3D components if the required accuracy is in the range of 500 µm and if surface finishing through subsequent post-processing is possible. Laser-post processing via laser polishing and laser functionalization was presented to be a versatile tool for the development of biocompatible surface. Similarly, the combination of SLM and subsequent laser surface post-processing is a powerful approach for the development of advanced and long operational lifetime VAD devices.

Acknowledgements

References

1. Kok, Y., X.P. Tan, P. Wang, M. Nai, N.H. Loh, E. Liu, and S.B. Tor, *Anisotropy and heterogeneity of microstructure and mechanical properties in metal additive manufacturing: A critical review.* Materials & Design, 2018. 139: p. 565-586.

2. Weng, F., C. Chen, and H. Yu, *Research status of laser cladding on titanium and its alloys: A review.* Materials & Design, 2014. 58: p. 412-425.

3. Carroll, B.E., R.A. Otis, J.P. Borgonia, J.-o. Suh, R.P. Dillon, A.A. Shapiro, D.C. Hofmann, Z.-K. Liu, and A.M. Beese, *Functionally graded material of 304L stainless steel and inconel 625 fabricated by directed energy deposition: Characterization and thermodynamic modeling.* Acta Materialia, 2016. 108: p. 46-54.

4. Melia, M.A., S.R. Whetten, R. Puckett, M. Jones, M.J. Heiden, N. Argibay, and A.B. Kustas, *High-throughput additive manufacturing and characterization of refractory high entropy alloys.* Applied Materials Today, 2020. 19: p. 100560.

5. Brenne, F. and T. Niendorf, *Load distribution and damage evolution in bending and stretch dominated Ti-6Al-4V cellular structures processed by selective laser melting.* International Journal of Fatigue, 2019. 121: p. 219-228.

6. Solheid, J., H.J. Seifert, and W. Pfleging, *Laser surface modification and polishing of additive manufactured metallic parts.* Procedia Cirp, 2018. 74: p. 280-284.

7. Solheid, J., A. Elkaseer, T. Wunsch, A. Charles, H.J. Seifert, and W. Pfleging. *Effect of process parameters on surface texture generated by laser polishing of additively manufactured Ti-6Al-4V.* in *Laser-based Micro-and Nanoprocessing XIV*. 2020. International Society for Optics and Photonics.

8. Solheid, J.S., S. Mohanty, M. Bayat, T. Wunsch, P.G. Weidler, H.J. Seifert, and W. Pfleging, *Laser polishing of additively manufactured Ti-6Al-4V: Microstructure evolution and material properties.* Journal of Laser Applications, 2020. 32(2): p. 022019.

9. Solheid, J.S., T. Wunsch, V. Trouillet, S. Weigel, T. Scharnweber, H.J. Seifert, and W. Pfleging, *Two-Step Laser Post-Processing for the Surface Functionalization of Additively Manufactured Ti-6Al-4V Parts.* Materials, 2020. 13(21): p. 4872.

10. Whitaker, M., *The history of 3D printing in healthcare.* The Bulletin of the Royal College of Surgeons of England, 2014. 96(7): p. 228-229.

11. Kawata, S., H.-B. Sun, T. Tanaka, and K. Takada, *Finer features for functional microdevices.* Nature, 2001. 412(6848): p. 697-698.

12. Jackson, R., S. Curran, P. Chambon, B. Post, L. Love, R. Wagner, B. Ozpineci, M. Chinthavali, M. Starke, and J. Green. *Overview of the Oak Ridge National Laboratory Advanced Manufacturing Integrated Energy Demonstration Project: case study of additive manufacturing as a tool to enable rapid innovation in integrated energy systems*. in *ASME 2016 international mechanical*

engineering congress and exposition. 2016. American Society of Mechanical Engineers Digital Collection.

13. Dai, Q., *China and the next production revolution.* 2017.

14. Sun, C. and G. Shang, *On Application of Metal Additive Manufacturing.* World Journal of Engineering and Technology, 2020. 9(1): p. 194-202.

15. Kumar, L.J. and C.K. Nair, *Current trends of additive manufacturing in the aerospace industry*, in *Advances in 3D printing & additive manufacturing technologies*. 2017, Springer. p. 39-54.

16. Hipolite, W. *Beijing University Unveils Enormous 3D Printed Aircraft Frames & More, Created with SLS Technology*. The Voice of 3D Printing/Additive Manufacturing 2017; Available from: https://3dprint.com/82169/3d-printed-aircraft-parts/.

17. Liu, R., Z. Wang, T. Sparks, F. Liou, and J. Newkirk, *Aerospace applications of laser additive manufacturing*, in *Laser additive manufacturing*. 2017, Elsevier. p. 351-371.

18. Seabra, M., J. Azevedo, A. Araújo, L. Reis, E. Pinto, N. Alves, R. Santos, and J.P. Mortágua, *Selective laser melting (SLM) and topology optimization for lighter aerospace componentes.* Procedia Structural Integrity, 2016. 1: p. 289-296.

19. Gibson, I., D.W. Rosen, and B. Stucker, *Sheet lamination processes*, in *Additive Manufacturing Technologies*. 2010, Springer: Boston, MA. p. 223-252.

20. Yang, L., K. Hsu, B. Baughman, D. Godfrey, F. Medina, M. Menon, and S. Wiener, *Introduction to Additive Manufacturing*, in *Additive Manufacturing of Metals: The Technology, Materials, Design and Production*. 2017, Springer International Publishing: Cham. p. 1-31.

21. Zäh, M.F. and S. Lutzmann, *Modelling and simulation of electron beam melting.* Production Engineering, 2010. 4(1): p. 15-23.

22. *SLM 280 - Robust Selective Laser Melting - Multiple Lasers and Process Stability for Demanding Applications*. 2021; Available from: www.slm-solutions.com/fileadmin/Content/Machines/SLM_R_280_Web.pdf.

23. Hofmann, D.C., S. Roberts, R. Otis, J. Kolodziejska, R.P. Dillon, J.-o. Suh, A.A. Shapiro, Z.-K. Liu, and J.-P. Borgonia, *Developing gradient metal alloys through radial deposition additive manufacturing.* Scientific reports, 2014. 4(1): p. 1-8.

24. Haase, C., F. Tang, M.B. Wilms, A. Weisheit, and B. Hallstedt, *Combining thermodynamic modeling and 3D printing of elemental powder blends for high-throughput investigation of high-entropy alloys–Towards rapid alloy screening and design.* Materials Science and Engineering: A, 2017. 688: p. 180-189.

25. Knoll, H., S. Ocylok, A. Weisheit, H. Springer, E. Jägle, and D. Raabe, *Combinatorial alloy design by laser additive manufacturing.* steel research international, 2017. 88(8): p. 1600416.

26. Hoffmann, P. and R. Dierken, *Laser Technology for Tool Production: Development of laser surface treatment–system technology and examples of application.* Laser Technik Journal, 2018. 15(3): p. 32-35.

27. Mahamood, R.M., E.T. Akinlabi, M. Shukla, and S. Pityana, *Scanning velocity influence on microstructure, microhardness and wear resistance performance of laser deposited Ti6Al4V/TiC composite.* Materials & design, 2013. 50: p. 656-666.

28. Lu, L., Y. Shi, C. Xu, G. Xu, J. Wang, and B. Xu, *The influence of pulse width and energy on temperature field in metal irradiated by ultrashort-pulsed laser.* Physics Procedia, 2012. 32: p. 39-47.

29. Gattass, R.R. and E. Mazur, *Femtosecond laser micromachining in transparent materials.* Nature Photonics, 2008. 2(4): p. 219-225.

30. Sugioka, K., *Ultrafast Laser Processing of Glass Down to the Nano-Scale.* Springer Series in Materials Science, 2010. 130: p. 279-293.

31. Sugioka, K., Y. Hanada, and K. Midorikawa, *Three-dimensional femtosecond laser micromachining of photosensitive glass for biomicrochips.* Laser & Photonics Reviews, 2010. 4(3): p. 386-400.

32.   Li, R., J. Liu, Y. Shi, L. Wang, and W. Jiang, *Balling behavior of stainless steel and nickel powder during selective laser melting process.* The International Journal of Advanced Manufacturing Technology, 2012. 59(9): p. 1025-1035.

33.   Niendorf, T., S. Leuders, A. Riemer, F. Brenne, T. Tröster, H.A. Richard, and D. Schwarze, *Functionally graded alloys obtained by additive manufacturing.* Advanced engineering materials, 2014. 16(7): p. 857-861.

34.   Nüsser, C., I. Wehrmann, and E. Willenborg, *Influence of intensity distribution and pulse duration on laser micro polishing.* Physics Procedia, 2011. 12: p. 462-471.

35.   Temmler, A., E. Willenborg, and K. Wissenbach. *Laser polishing*. in *Laser Applications in Microelectronic and Optoelectronic Manufacturing (LAMOM) XVII*. 2012. International Society for Optics and Photonics.

36.   Kumari, R., T. Scharnweber, W. Pfleging, H. Besser, and J.D. Majumdar, *Laser surface textured titanium alloy (Ti–6Al–4V)–Part II–Studies on bio-compatibility.* Applied Surface Science, 2015. 357: p. 750-758.

37.   Kumari, R., W. Pfleging, H. Besser, and J.D. Majumdar, *Microstructure and corrosion behavior of laser induced periodic patterned titanium based alloy.* Optics & Laser Technology, 2019. 116: p. 196-213.

38.   Marquiori, D.S., P.C. Florentino, S.Y. Araki, I.K. Fujita, R.L.d.O. Basso, A. Babetto, B.C. Bonse, J.R. Moro, T. Leao, A.J. Andrade, and E.G.P. Bock, *Tribology and Crystallinity in pivot bearings of Ventricular Assist Devices.* The Academic Society Journal, 2020. 4(1): p. 52-62.

39.   Hofmann, D.C., J. Kolodziejska, S. Roberts, R. Otis, R.P. Dillon, J.-O. Suh, Z.-K. Liu, and J.-P. Borgonia, *Compositionally graded metals: A new frontier of additive manufacturing.* Journal of Materials Research, 2014. 29(17): p. 1899-1910.

40.   Pouzet, S., P. Peyre, C. Gorny, O. Castelnau, T. Baudin, F. Brisset, C. Colin, and P. Gadaud, *Additive layer manufacturing of titanium matrix composites using the direct metal deposition laser process.* Materials Science and Engineering: A, 2016. 677: p. 171-181.

41.   Li, G.-C., J. Li, X.-J. Tian, X. Cheng, B. He, and H.-M. Wang, *Microstructure and properties of a novel titanium alloy Ti-6Al-2V-1.5 Mo-0.5 Zr-0.3 Si manufactured by laser additive manufacturing.* Materials Science and Engineering: A, 2017. 684: p. 233-238.

42.   Dezfoli, A.R.A., W.-S. Hwang, W.-C. Huang, and T.-W. Tsai, *Determination and controlling of grain structure of metals after laser incidence: Theoretical approach.* Scientific reports, 2017. 7(1): p. 1-11.

43.   Tang, Y., Y. Zhang, and Y. Liu, *Numerical and experimental investigation of laser additive manufactured Ti2AlNb-based alloy.* Journal of Alloys and Compounds, 2017. 727: p. 196-204.

44.   Ye, Y., Q. Wang, J. Lu, C. Liu, and Y. Yang, *High-entropy alloy: challenges and prospects.* Materials Today, 2016. 19(6): p. 349-362.

45.   Dobbelstein, H., E.L. Gurevich, E.P. George, A. Ostendorf, and G. Laplanche, *Laser metal deposition of compositionally graded TiZrNbTa refractory high-entropy alloys using elemental powder blends.* Additive Manufacturing, 2019. 25: p. 252-262.

46.   Dobbelstein, H., E.L. Gurevich, E.P. George, A. Ostendorf, and G. Laplanche, *Laser metal deposition of a refractory TiZrNbHfTa high-entropy alloy.* Additive Manufacturing, 2018. 24: p. 386-390.